

Relativistic capture of dark matter by electrons in neutron stars

Aniket Joglekar,^{1,*} Nirmal Raj,^{2,†} Philip Tanedo,^{1,‡} and Hai-Bo Yu^{1,§}

¹*Department of Physics and Astronomy, University of California, Riverside, California 92521, USA*

²*TRIUMF, 4004 Wesbrook Mall, Vancouver, BC V6T 2A3, Canada*

(Dated: January 16, 2022)

Dark matter can capture in neutron stars and heat them to observable luminosities. We study relativistic scattering of dark matter on highly degenerate electrons. We develop a Lorentz invariant formalism to calculate the capture probability of dark matter that accounts for the relativistic motion of the target particles and Pauli exclusion principle. We find that the actual capture probability can be five orders of magnitude larger than the one estimated using a nonrelativistic approach. For dark matter masses 10 eV–10 PeV, neutron star heating complements and can be more sensitive than terrestrial direct detection searches. The projected sensitivity regions exhibit characteristic features that demonstrate a rich interplay between kinematics and Pauli blocking of the DM–electron system. Our results show that old neutron stars could be the most promising target for discovering leptophilic dark matter.

Dark matter (DM) makes up more than 80% of the mass in the universe, but its identity remains largely unknown. There has been growing interest in signals of DM capture in compact stars [1–25]. In particular, neutron stars have super-nuclear densities that make them intriguing DM detectors. Incident DM particles are accelerated by the steep gravitational potential and may deposit their kinetic energy as heat via scattering with individual stellar constituents [26–35]¹. If radio telescopes observe a nearby old pulsar, upcoming infrared telescopes may measure the stellar luminosity and detect this DM kinetic heating. This search is largely independent of the details of DM interactions with Standard Model particles and thus sensitive to numerous scenarios of DM that are otherwise inaccessible to terrestrial detectors [26–28, 35].

The electron–DM portal is a well-motivated scenario that is crucial for light DM detection; see [37]. There have been a wide-ranging suite of experimental efforts in this new direction [38–46]. In this *Letter*, we show that despite making up only $\sim 3 \times 10^{-3} \%$ of the stellar mass, the electrons in a neutron star are excellent targets for capturing DM. Neutron star heating can search for DM masses and couplings that greatly exceed the limits set by the Earth-based direct detection experiments.

Electrons in the neutron star are ultrarelativistic, highly degenerate and are moving in random directions, while DM particles approaching a neutron star are quasirelativistic with star escape velocity $v_{\text{esc}} \sim 0.6$. Because each DM–electron center of momentum frame is distinct and highly boosted from the neutron star frame, the conventional formalism, developed for nonrelativistic targets, is invalid in calculating the capture probability.

For the system we consider, it is necessary to specify the key scattering ingredients in different reference frames. The DM–electron scattering cross section is most conveniently expressed in the center of momentum frame of each DM–electron pair, while the target Fermi–Dirac distributions are best defined in the neutron star frame.

We develop a manifestly Lorentz invariant formalism to express the capture probability per DM particle in the neutron star in terms of the kinematic ingredients discussed above. It incorporates Pauli blocking and other capture conditions so that one may integrate over the phase space available for DM capture. We apply this formalism to two benchmark DM scenarios and estimate sensitivities on model parameters from neutron star heating. The first assumes a contact operator to model DM–electron interactions. The second contains a light mediator particle with fixed in-medium effective masses of 1 keV and 10 MeV, well below the Fermi momentum.

We find that the actual electron capture probability can be a factor of $(p_F/m_e)^2 \sim 10^5$ larger than the estimate using a nonrelativistic approach. For DM masses between 10 eV–10 PeV, the neutron star constraints are stronger than current limits from DM direct detection experiments in most of the mass range including the light DM regime. In particular, neutron star heating could be the most promising method to discover leptophilic DM.

Lorentz-invariant capture. A DM particle is bound to a neutron star if it loses its halo kinetic energy $E_{\text{halo}} = m_\chi v_h^2/2$ by scattering within the star. For N_{hit} scatters that deposit average energy $\langle \Delta E \rangle$, capture occurs when $N_{\text{hit}} \langle \Delta E \rangle > E_{\text{halo}}$. We take the DM velocity in the halo to be $v_h = 220$ km/s. The rate of kinetic energy deposition is $\dot{K} = (\gamma_{\text{esc}} - 1) \dot{m}_\chi f$, where $\gamma_{\text{esc}} = (1 - v_{\text{esc}}^2)^{-1/2}$, $\dot{m}_\chi \sim 10^{25}$ GeV/s is the mass capture rate, and f is the optical depth of DM in the star such that the probability for a transiting DM particle to capture is given by $1 - e^{-f}$; as we will be concerned with the optically thin limit, we treat f as the capture probability. This process equilibrates on galactic timescales and the deposited energy is radiated as heat. The resulting blackbody tem-

* aniket@ucr.edu

† nrnj@triumf.ca

‡ flip.tanedo@ucr.edu

§ haiboyu@ucr.edu

¹ If DM were made of primordial black holes, they could be slowed down and captured in the stellar medium via the effect of dynamical friction, see e.g. [36]

perature is $T_\star \approx 1600 f^{1/4}$ K [26, 27]. For $f = 1$ this is $\mathcal{O}(10)$ higher than that of a 10^9 year-old neutron star that is not heated by DM [47, 48], unless the neutron star undergoes rotochemical heating that depends on the initial period and nuclear modelling [31]. The key step to accurately study DM signals from neutron star heating is to calculate the capture probability per DM particle, f .

To develop a formalism for f that is manifestly Lorentz invariant, we first consider the frame-invariant number of scattering events ($d\nu$) constructed in the DM rest frame in which the cross section and relative velocity can be properly defined [49]:

$$d\nu = (d\sigma \cdot v \cdot dn_T \cdot \Delta t \cdot dn_\chi \cdot \Delta V)_{\text{DM}}, \quad (1)$$

where $d\sigma$ is the cross section, v is the relative velocity, dn_χ , dn_T are infinitesimal DM and target number densities respectively, ΔV denotes interaction volume and Δt transit time; all evaluated in the DM frame. Since $d\nu$ and $dn_\chi \Delta V$ are Lorentz invariant, so is their ratio $df = d\nu / (\Delta V dn_\chi) = (d\sigma \cdot v \cdot dn_T \cdot \Delta t)_{\text{DM}}$, the infinitesimal scattering probability. So we can write f in terms of the corresponding variables in the neutron star frame $df = (d\sigma \cdot v \cdot dn_T \cdot \Delta t)_{\text{NS}}$. For a given target 4-momentum $p_\mu = (E_p, \vec{p})_{\text{NS}}$ and DM 4-momentum $k_\mu = (E_k, \vec{k})_{\text{NS}}$ in the neutron star frame, there exists a relation, $(d\sigma \cdot v)_{\text{NS}} = (d\sigma)_{\text{DM}}(v_{\text{Møl}})_{\text{NS}}$, where $(v_{\text{Møl}})_{\text{NS}} = \sqrt{(p \cdot k)^2 - m_T^2 m_\chi^2} / (E_p E_k)_{\text{NS}}$ is the Møller velocity in the neutron star frame. From this and using the fact that the cross section is invariant under boost along the collision axis, i.e., $(d\sigma)_{\text{DM}} = (d\sigma)_{\text{CM}}$, where

“CM” denotes the center of momentum frame, we obtain an expression for df ,

$$df = \left(\frac{d\sigma}{d\Omega} \right)_{\text{CM}} d\Omega_{\text{CM}} (v_{\text{Møl}} dn_T \Delta t)_{\text{NS}}, \quad (2)$$

where $d\Omega_{\text{CM}} = d\cos\psi d\alpha$, for CM polar and azimuthal angles ψ and α . Note that the last term in parentheses is Lorentz invariant. For what follows, we will suppress subscript “NS” when referencing a variable in the neutron star frame, except in a few instances to avoid confusion.

Pauli blocking and phase space. To evaluate f in Eq. 2, we need to perform the phase-space integral over $d\Omega_{\text{CM}} dn_T$. However, not all parts of the phase space are allowed to interact due to the Pauli exclusion principle, which requires the target particle to be knocked out of its Fermi sea in order to interact. Making use of the Lorentz invariance of f , we analyze the Pauli blocking condition in the neutron star frame, where the Fermi surface is spherical. The condition can be expressed in the form of the Heaviside step function $\Theta(\Delta E + E_p - E_F)$, where E_F is the Fermi energy and ΔE is the energy transferred to the target in the collision; both of them are in the neutron star frame. Note that ΔE is related to the momentum transfer in the CM frame (\vec{q}_{CM}) as $\Delta E = \vec{\beta}_{\text{CM}} \cdot \vec{q}_{\text{CM}} / \sqrt{1 - \beta_{\text{CM}}^2}$, where $\vec{\beta}_{\text{CM}} = (\vec{p} + \vec{k}) / (E_p + E_k)$ is the boost from the neutron star to the CM frame. Finally, we must satisfy the capture condition, $N_{\text{hit}} \langle \Delta E \rangle > E_{\text{halo}}$. This is done by summing over N_{hit} in a conservative way to ensure at least E_{halo} is transferred to the neutron star during transit of a DM particle through it. This accounts for the case when many scatters with smaller ΔE are more efficient than a single scatter with large ΔE . Putting these together, we have

$$f = \sum_{N_{\text{hit}} \in \mathbb{Z}} \frac{\langle n_T \rangle \Delta t}{N_{\text{hit}}} \int d\Omega_{\text{NS}} \int_0^{p_F} d|\vec{p}| \frac{|\vec{p}|^2}{V_F} v_{\text{Møl}} \int d\Omega_{\text{CM}} \left(\frac{d\sigma}{d\Omega} \right)_{\text{CM}} \Theta(\Delta E + E_p - E_F) \Theta\left(\frac{E_{\text{halo}}}{N_{\text{hit}} - 1} - \Delta E\right) \Theta\left(\Delta E - \frac{E_{\text{halo}}}{N_{\text{hit}}}\right), \quad (3)$$

where $\langle n_T \rangle$ is the average number density of the target species in the neutron star core, $V_F = 4\pi p_F^3/3$ is the Fermi volume, and $dn_T = |\vec{p}|^2 d|\vec{p}| d\Omega_{\text{NS}}/V_F$. We take $\langle n_T \rangle = 3M_\star Y_T / 4\pi m_n R_\star^3$, where Y_T is the target’s volume-averaged number per nucleon, M_\star is the mass of the neutron star and R_\star its radius. For the constituents $\{e^-, \mu^-, p^+, n\}$, we take their corresponding $Y_T = \{0.06, 0.02, 0.07, 0.93\}$ and Fermi momentum $p_F = \{146, 50, 160, 373\}$ in MeV as calculated in [33] using the unified equation of state (EoS) BSk24 of the Brussels-Montreal model [50]. We take $M_\star = 1.5 M_\odot$ and $R_\star = 12.6$ km to be consistent with the calculation of Y and p_F in [33].

As an approximation, we take the volume-averaged values for $\langle n_T \rangle$, Y_T and p_F over the core. We have estimated

the maximum deviation in our projected cut-off bounds possible due to radial variations of those quantities and different choices of EoS [29, 33, 50]. These deviations may at most lead to an $\mathcal{O}(1)$ change in our projected sensitivities for neutrons and electrons. Detailed discussion of these variations is deferred to the section on uncertainties in the end. As we will also show later, projected bounds due to electrons in neutron star could be several orders of magnitude stronger than DM direct detection limits, thus a small $\mathcal{O}(1)$ change does not affect our main results.

We recover the usual form of f from Eq. 3 for non-relativistic targets. As $p_F \rightarrow 0$, the differential cross section becomes independent of p_μ and $v_{\text{Møl}} \rightarrow v_{\text{esc}}$, also the Pauli blocking step function $\rightarrow 1$. These im-

ply $\int |\vec{p}|^2 d|\vec{p}| d\Omega_{\text{NS}} / V_F \rightarrow 1$. Assuming that a single scatter deposits at least E_{halo} , Eq. 3 gives $f = \int d\Omega_{\text{CM}} (d\sigma/d\Omega)_{\text{CM}} / (\langle n_T \rangle v_{\text{esc}} \Delta t)^{-1}$, a well-known result, where the denominator is the geometric cross section.

DM model with a heavy mediator. We apply our framework to estimate sensitivities from neutron star heating for representative DM models and compare them with limits from DM direct detection experiments. We assume the DM candidate is a Dirac fermion (χ) that couples to Standard Model fermions (ξ) through an effective vectorial operator, $(\bar{\chi}\gamma_\mu\chi)(\bar{\xi}\gamma^\mu\xi)/\Lambda^2$. We explore spin-0 DM and other interactions structures in a companion paper [55]. The sensitivity of the proposed search is an upper limit on Λ .

Fig. 1 (left) shows our projected sensitivities to the cutoff scale Λ vs the DM mass m_χ , obtained numerically, for the target fermions $\xi = e^-, \mu^-, p^+$ and n . The upper boundaries correspond to $f = 1$, or signal temperature $T_\star = 1600$ K. Stronger sensitivities could be obtained for $f < 1$, corresponding to smaller T_\star .

The plot demonstrates three distinct regimes: (i) For $m_\chi \gtrsim 1$ PeV, the sensitivities decrease as the DM mass increases further. In this region, DM becomes so massive that multiple scatterings ($N_{\text{hit}} > 1$) are required for successful capture, suppressing the capture probability, as indicated in Eq. 3. (ii) For $p_F \lesssim m_\chi \lesssim 1$ PeV, there are plateaus insensitive to the DM mass. In this mass range, the momentum transfer is typically larger than the Fermi momentum and Pauli blocking is unimportant. In addition, the cross section is almost independent of the DM mass. Thus the projected upper limits on Λ are nearly constant over m_χ . The electron capture sensitivity to Λ is more than a factor 10 stronger than the one estimated with a nonrelativistic treatment [33]. (iii) For light DM, $m_\chi \lesssim p_F$, the sensitivities decrease for all targets, due to a combined effect of Pauli blocking and suppression of the cross section, as we will discuss later. In this regime, the nonrelativistic treatment of the electrons overestimates the capture probability.

For comparison, we show constraints from DM direct direction experiments based on both electron [38, 43, 51, 52] and nuclear recoils [42, 44, 53, 54]. Remarkably, for light DM with $m_\chi \sim 10$ MeV–10 GeV, the neutron star bound on Λ can be a factor of 100 stronger than electron recoil limits. Furthermore, neutron star heating may probe a broader DM mass range not covered by direct detection for electron recoils, as well as nuclear recoils [27]. If DM couples to both electrons and nucleons equally, the limit on Λ will be mainly set by DM–neutron/proton scatterings. On the other hand, for leptophilic DM, capture by electrons is the strongest mode of neutron star heating for $m_\chi > p_F$. We have checked that this is true even after taking into account loop-induced interactions of leptophilic DM with nucleons, in contrast to earlier results using the nonrelativistic approach [33].

To further understand the scaling features in Fig. 1 (left), we explore the scattering kinematics in more de-

tail. The scattering cross section scales as $(d\sigma/d\Omega)_{\text{CM}} \propto m_\chi^2 E_p^2 / (s\Lambda^4)$, where E_p is the target energy in the neutron star frame and s is the Mandelstam variable. In the nonrelativistic limit, $E_p \approx m_T$ and $s \approx (m_\chi + m_T)^2$, and $(d\sigma/d\Omega)_{\text{CM}}$ reduces to the well-known form $(m_\chi m_T)^2 / (m_\chi + m_T)^2 \Lambda^4$. The DM energy and momentum in the neutron star frame are $E_k = \gamma_{\text{esc}} m_\chi$ and $|\vec{k}| = v_{\text{esc}} \gamma_{\text{esc}} m_\chi$ respectively, where $\gamma_{\text{esc}} = 1.24$ and $v_{\text{esc}} = 0.6$. For the electrons, these are $E_p \approx p_F$ and $|\vec{p}| = p_F$ respectively, as the electron Fermi momentum 146 MeV is much larger than its mass 0.51 MeV, i.e., electrons in the neutron star core are ultrarelativistic.

Consider the heavy DM mass region, where $m_\chi \gg p_F$ and Pauli blocking is unimportant. For the DM–electron system, $s = (E_k + E_p)^2 - (\vec{k} + \vec{p})^2 \approx E_k^2 - k^2 = m_\chi^2$. Thus, the scattering cross section scales as $(d\sigma/d\Omega)_{\text{CM}} \propto p_F^2 / \Lambda^4$. Compared to the nonrelativistic approach in the neutron star frame, where $(d\sigma/d\Omega)_{\text{CM}} \propto m_e^2 / \Lambda^4$, the actual cross section is a factor of $(p_F/m_e)^2 \sim 10^5$ larger. Thus, the actual neutron star sensitivity on Λ is more than one order of magnitude stronger than estimated previously with nonrelativistic approach [33], as indicated in Fig. 1 (left). For the other targets, $(p_F/m_T)^2 < 1$, the nonrelativistic approximation is valid.

For light DM $m_\chi \ll p_F$, the reach shown in Fig. 1 (left) scales as $\Lambda \propto m_\chi^{3/4}$ for all targets, which can be understood as follows. For the nonrelativistic targets n, p^+ and μ^- , DM energy loss has a weak dependence on the scattering angle, and the Pauli blocking factor scales as m_χ . Moreover, the cross section $\propto m_\chi^2 / \Lambda^4$. Thus, the capture probability $f \propto m_\chi^3 / \Lambda^4$. For the ultrarelativistic electrons, $s = (E_k + E_p)^2 - (\vec{k} + \vec{p})^2 \approx 2(E_k E_p - \vec{k} \cdot \vec{p}) \propto m_\chi p_F$, resulting in $(d\sigma/d\Omega)_{\text{CM}} \propto m_\chi p_F / \Lambda^4$. Since the energy loss only occurs for CM frame forward scatterings in this case, there is an additional suppression in the phase space $\propto m_\chi$, which is not present for the nonrelativistic targets. Thus the Pauli blocking factor scales as m_χ^2 , and we again have $f \propto m_\chi^3 / \Lambda^4$ for the electron target. Note the nonrelativistic approach for electrons overestimates the sensitivity for $m_\chi < m_e$, because it does not take into account the fact that it is much harder to transfer energy to an ultrarelativistic electron than one at rest.

DM model with a light mediator. We consider a DM model with a light vector mediator and corresponding scattering cross section

$$\left(\frac{d\sigma}{d\Omega} \right)_{\text{CM}} \propto \frac{g_\chi^2 g_T^2 m_\chi^2 E_p^2}{s(m_{\text{eff}}^2 + |\vec{q}|_{\text{CM}}^2)}, \quad (4)$$

where g_χ, g_T are the mediator’s couplings to DM and the target respectively, m_{eff} is the in-medium effective mediator mass. This effective mass is simply the mediator mass $m_{\text{eff}} = m_{\text{med}}$, when m_{med} is larger than the inverse of the Debye length that we estimate as [56–62]

$$\lambda_D^{-1} \sim e \sqrt{\frac{n_e}{T_{\text{eff}}}} \sim e \sqrt{\frac{n_e}{p_F}} \approx 10 \text{ MeV}, \quad (5)$$

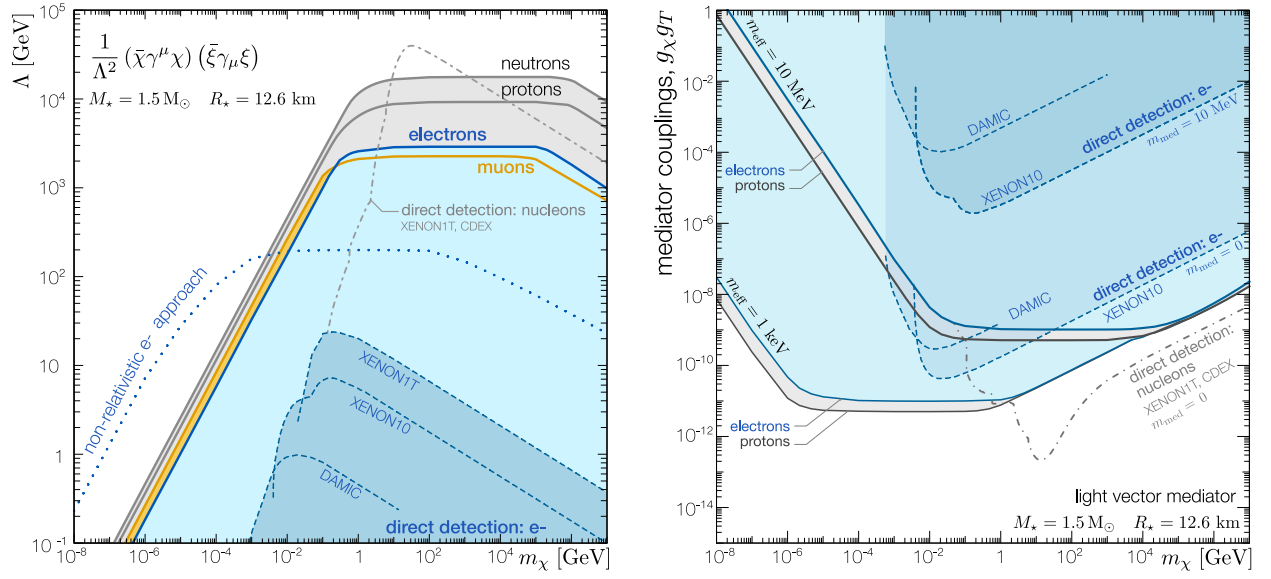


FIG. 1. Projected sensitivities from neutron star heating for vectorial interactions of Dirac DM with Standard Model fermions (solid), together with Earth-based direct detection constraints (dashed) [38, 42–44, 51–54]. *Left:* A heavy mediator scenario characterized by a cutoff scale Λ for capture by various neutron star constituents. The dotted line shows a non-relativistic calculation that underestimates (overestimates) the sensitivity above (below) the electron Fermi energy (electron mass). *Right:* A light mediator scenario for the capture by electrons and protons, with sensitivities displayed for the product of the mediator’s couplings to DM and Standard Model fermions. The direct detection constraints here assume the mediator mass to be massless or 10 MeV; the massive mediator lines are recast using the experimental bounds corresponding to the form factor $F_{\text{DM}} = 1$ [38, 43, 51, 52]. In both panels, the colored regions correspond to $f = 1$ ($T_\star = 1600$ K) as estimated from Eq. 3. Projected sensitivities are stronger if we take lower f , i.e. lower T_\star , corresponding to longer observation times.

where T_{eff} is the effective temperature for ThomasFermi screening; $T_{\text{eff}} \approx p_F$. In deriving potential constraints from neutron stars, we take $m_{\text{eff}} = \lambda_D^{-1} \approx 10$ MeV. For reference, we also show the reach for $m_{\text{eff}} = 1$ keV.

Fig. 1 (right) shows our sensitivities to $g_\chi g_T$ for electron and proton targets. We compare to direct detection limits for DM with massless and 10 MeV mediators. For mediators in this range, we estimate that the neutron star heating reach is represented by the $m_{\text{eff}} = 10$ MeV curves. For leptophilic mediators with a mass of 10 MeV, the neutron star reach for $g_\chi g_T$ is orders of magnitudes stronger with respect to current bounds from terrestrial direct detection probes for the entire range of accessible DM masses. For the limit of massless mediators, the neutron star kinetic heating reach for $m_{\text{eff}} = 10$ MeV is stronger than Earth-based detectors for DM masses lighter than 1 MeV and heavier than 100 GeV. If DM couples to e^- and p^+ equally, the combined bounds on $g_\chi g_T$ would be at most stronger by a factor of $\sqrt{2}$.

As shown in Fig. 1 (right), the projected reach changes slope when $m_\chi \approx m_{\text{eff}}$ for both electron and proton targets. For $m_\chi \ll m_{\text{eff}} \ll p_F$, as seen from Eq. 4, $f \propto g_\chi^2 g_T^2 m_\chi^3 / m_{\text{eff}}^4$ and the reach on $g_\chi g_T \propto m_\chi^{-3/2}$. This is similar to the heavy-mediator model in the region of $m_\chi \ll p_F$. While for $m_\chi > m_{\text{eff}}$, one finds plateaus where the reach is constant with respect to m_χ , and they extend towards a lower DM mass range, compared to the heavy-mediator model. As m_χ drops below p_F , Pauli

blocking suppresses the scattering phase space and reduces the capture probability. However, for the light-mediator model, the scattering cross section is enhanced by a small momentum transfer. These two competing effects reach a balance, resulting in the plateaus shown in Fig. 1 (right).

To see this, observe that in Eq. 4, the momentum transfer $|\vec{q}|_{\text{CM}}$ below m_{eff} can not significantly enhance the differential cross section. Consider the expression for $|\vec{q}|_{\text{CM}}^2 = 2|\vec{k}|_{\text{CM}}^2(1 - \cos \psi)$, where ψ is the scattering angle in the CM frame. Let $|\vec{q}|_{\text{CM}} \sim m_{\text{eff}}$ for $\psi = \psi_0$. Neglecting sub-dominant contributions to Eq. 3 from the region $\psi > \psi_0$, the phase-space integral is $\int_{\cos \psi_0}^1 d \cos \psi' \sim m_{\text{eff}}^2 / |\vec{k}|_{\text{CM}}^2$. The allowed phase space is also suppressed in the magnitude of $|\vec{p}|$ as $|\vec{q}|_{\text{CM}} / p_F \sim m_{\text{eff}} / p_F$. Putting these factors together with Eq. 4, we have

$$f \propto \frac{g_\chi^2 g_T^2 m_\chi^2 E_p^2}{s m_{\text{eff}}^4} \cdot \frac{m_{\text{eff}}^2}{|\vec{k}|_{\text{CM}}^2} \cdot \frac{m_{\text{eff}}}{p_F} \propto \frac{g_\chi^2 g_T^2}{p_F m_{\text{eff}}}, \quad (6)$$

where we use $s|\vec{k}|_{\text{CM}}^2 \propto m_\chi^2 E_p^2$. Thus, f is not sensitive to m_χ in this region. As we increase m_χ , the cross section is suppressed by a high momentum transfer, and multiple scatterings become relevant; both effects lead to a small capture probability, resulting in weak reaches.

We note that for $m_\chi > m_{\text{eff}}$ it is possible for incident DM to emit a mediator via bremsstrahlung and slow down, however the rate for this is expected to be negligi-

ble given the small g_χ couplings to which we are sensitive (Fig. 1) and the phase space suppression with respect to the scattering cross section.

Uncertainties. In this section, we estimate the maximum deviation possible in our results for the projected reach of Λ , due to the radial variation of baryon density, BSk functional, M_\star , and R_\star . The exact calculation of these effects is beyond the scope of this paper and is deferred to future work. We also note that the BSk functionals from [50] used in this paper only take into account the four target species considered above as neutron star constituents, and neglect the possible presence of any exotic phases of matter.

From Eq. 3, we observe that possible sources of uncertainties in our projected sensitivities are the baryon density, the p_F -dependence of the phase space integral, Y_T and Δt . Given an equation of state functional, and a (M_\star, R_\star) pair predicted by it, the baryon density sets the values of Y_T and p_F . The baryon density itself varies in the core as a function of distance from the center. However, by significantly varying M_\star and R_\star , a wide range of average baryon densities for the core can be obtained. This range is greater than the deviation from average baryon density within the core for a fixed configuration. This is because typically, the baryon number density remains relatively constant for at least half to two thirds of the radius.

Hence, to estimate the maximum variation in our results, we consider two extreme average densities, allowed amongst all the valid M_\star and R_\star configurations of BSk22, BSk24, BSk25 and BSk26 functionals. Consequently, for high mass ($2.16 M_\odot$) – small radius (11 km) configuration, the average core baryon density is about 0.61 fm^{-3} and for low mass ($0.3 M_\odot$) – large radius (13 km) configuration, it is about 0.05 fm^{-3} [33, 50]. For the dense configurations, the central baryon number density can go as high as 0.95 fm^{-3} . Therefore, we consider the range 0.05 fm^{-3} to 0.95 fm^{-3} of the baryon number density for our uncertainty estimation. The corresponding ranges of values for Y_T and p_F for each target species can be obtained from [50]. Thus, we find that the baryon density, Y_T , and p_F vary by a factor of < 5 with respect to the ones considered in our results.

Substituting all these quantities in Eq. 3 and taking $1/4^{\text{th}}$ power, we estimate the width of uncertainty bands for the projected sensitivities on our EFT cutoff. For all species, the upper end of the band is a factor of 1.8 times the values in the left panel of Fig. 1. The only exception is sensitivity to electron scattering in the heavy DM region, where the band extends up to 3 times the reach in Λ shown. The lower end of the band differs according to the target species. For neutrons it is at most a factor 1.7 lower than the values in Fig. 1, while for electrons it could be a factor of at most 2.5. If the central density of the neutron star configuration falls below that needed for having non-zero muon abundance, then the DM capture via muons is not possible. For configurations with sufficiently low densities, i.e., core average density below

0.12 fm^{-3} , the muon bounds are significantly weakened.

The neutron and electron bands are well separated in the heavy DM region, but overlap in the light DM region. For configurations with densities higher than those used in Fig. 1, the electron bound in heavy DM region will move closer to the neutron bound. This is because higher Fermi momentum helps heavy DM capture by electrons unlike in the case of nucleon targets. For sufficiently high densities, electrons maintain their dominance over muons in the heavy DM region for the same reason. For light DM, the bands for electrons and neutrons overlap, with neutrons generally exhibiting slightly stronger bound compared to electrons for any given configuration. Muon targets provide higher sensitivity compared to electrons in the light DM region as seen in the left panel of Fig. 1. For configurations with sufficiently high baryon density, the electron and muon bounds remain comparable. However, for configurations with low baryon density, where the abundance of electrons in the central region strongly dominates over that of muons, the tables are turned and electrons start dominating in the light DM region as well.

We have assumed $\Delta t = 2R_\star$. The number of DM particles following the paths with $\Delta t > 2R_\star$ are an $\mathcal{O}(1)$ fraction of the total flux through the star. The resultant underestimation of the capture efficiency is of course mitigated by the overestimation from shorter paths with $\Delta t < 2R_\star$ by a small $\mathcal{O}(1)$ factor. Some target species like protons or muons only capture the DM up to a certain radial distance inside the core for certain configurations of M_\star and R_\star , shrinking Δt by a small $\mathcal{O}(1)$ factor. In the end, the uncertainty resulting from these factors in the sensitivity to Λ is suppressed since $\Lambda \propto f^{1/4}$. We find that the uncertainty in our reach in Λ due to the variation in Δt is at most $\mathcal{O}(10\%)$.

Conclusions. We have studied relativistic capture of DM by electrons in a neutron star and developed a formalism to calculate the capture probability. It is manifestly Lorentz invariant and incorporates relativistic scattering kinematics, Pauli blocking, and the effect of multiple DM–electron scatters during stellar transit. We further applied the formalism to explore the sensitivities to parameter space of two benchmark DM scenarios and compared them with direct detection limits. The Lorentz-invariant capture probability can be five orders of magnitude larger than the traditional non-relativistic approach. This makes neutron star heating one of the most promising testing grounds for probing leptophilic DM models. In the future, we could apply our formalism to other DM models [27, 63–65] and different capture scenarios [15, 35, 66]. It is also interesting to investigate the discovery potential of old neutron stars using upcoming radio telescopes and infrared surveys, see., e.g, [67–70].

ACKNOWLEDGMENTS

We thank Nicole Bell, Joe Bramante, David Morrissey, Tongyan Lin, and Ethan Villarama for useful discussions. This work is supported by the U. S. Department of Energy under Grant No. de-sc 0008541 (AJ, PT, HBY), and the Natural Sciences and Engineering Research Council of Canada (NSERC) (NR). TRIUMF receives federal

funding via a contribution agreement with the National Research Council Canada. This work was also performed in part at the Aspen Center for Physics (NR, PT), which is supported by National Science Foundation grant PHY-1607611. A part of this work was also completed at Kavli Institute for Theoretical Physics (AJ, HBY), which is supported in part by the National Science Foundation under Grant No. NSF PHY-1748958.

-
- [1] I. Goldman and S. Nussinov, Phys. Rev. **D40**, 3221 (1989).
 - [2] A. Gould, B. T. Draine, R. W. Romani, and S. Nussinov, Phys. Lett. **B238**, 337 (1990).
 - [3] C. Kouvaris, Phys. Rev. **D77**, 023006 (2008), arXiv:0708.2362 [astro-ph].
 - [4] G. Bertone and M. Fairbairn, Phys. Rev. **D77**, 043515 (2008), arXiv:0709.1485 [astro-ph].
 - [5] A. de Lavallaz and M. Fairbairn, Phys. Rev. **D81**, 123521 (2010), arXiv:1004.0629 [astro-ph.GA].
 - [6] C. Kouvaris and P. Tinyakov, Phys. Rev. **D82**, 063531 (2010), arXiv:1004.0586 [astro-ph.GA].
 - [7] S. D. McDermott, H.-B. Yu, and K. M. Zurek, Phys. Rev. **D85**, 023519 (2012), arXiv:1103.5472 [hep-ph].
 - [8] C. Kouvaris and P. Tinyakov, Phys. Rev. Lett. **107**, 091301 (2011), arXiv:1104.0382 [astro-ph.CO].
 - [9] T. Guver, A. E. Erkoca, M. Hall Reno, and I. Sarcevic, JCAP **1405**, 013 (2014), arXiv:1201.2400 [hep-ph].
 - [10] J. Bramante, K. Fukushima, and J. Kumar, Phys. Rev. **D87**, 055012 (2013), arXiv:1301.0036 [hep-ph].
 - [11] N. F. Bell, A. Melatos, and K. Petraki, Phys. Rev. **D87**, 123507 (2013), arXiv:1301.6811 [hep-ph].
 - [12] J. Bramante, K. Fukushima, J. Kumar, and E. Stopnitzky, Phys. Rev. **D89**, 015010 (2014), arXiv:1310.3509 [hep-ph].
 - [13] C. Kouvaris and P. Tinyakov, Phys. Rev. **D83**, 083512 (2011), arXiv:1012.2039 [astro-ph.HE].
 - [14] M. McCullough and M. Fairbairn, Phys. Rev. **D81**, 083520 (2010), arXiv:1001.2737 [hep-ph].
 - [15] B. Bertoni, A. E. Nelson, and S. Reddy, Phys. Rev. **D88**, 123505 (2013), arXiv:1309.1721 [hep-ph].
 - [16] M. Angeles Perez-Garcia and J. Silk, Phys. Lett. **B744**, 13 (2015), arXiv:1403.6111 [astro-ph.SR].
 - [17] J. Bramante, Phys. Rev. Lett. **115**, 141301 (2015), arXiv:1505.07464 [hep-ph].
 - [18] P. W. Graham, S. Rajendran, and J. Varela, Phys. Rev. **D92**, 063007 (2015), arXiv:1505.04444 [hep-ph].
 - [19] M. Cerneno, M. A. Perez-Garcia, and J. Silk, Phys. Rev. **D94**, 063001 (2016), arXiv:1607.06815 [astro-ph.HE].
 - [20] R. Krall and M. Reece, Chin. Phys. **C42**, 043105 (2018), arXiv:1705.04843 [hep-ph].
 - [21] P. W. Graham, R. Janish, V. Narayan, S. Rajendran, and P. Riggins, Phys. Rev. **D98**, 115027 (2018), arXiv:1805.07381 [hep-ph].
 - [22] D. McKeen, A. E. Nelson, S. Reddy, and D. Zhou, Phys. Rev. Lett. **121**, 061802 (2018), arXiv:1802.08244 [hep-ph].
 - [23] J. F. Acevedo and J. Bramante, Phys. Rev. **D100**, 043020 (2019), arXiv:1904.11993 [hep-ph].
 - [24] R. Janish, V. Narayan, and P. Riggins, Phys. Rev. **D100**, 035008 (2019), arXiv:1905.00395 [hep-ph].
 - [25] N. F. Bell, G. Busoni, S. Robles, and M. Virgato, (2020), arXiv:2004.14888 [hep-ph].
 - [26] M. Baryakhtar, J. Bramante, S. W. Li, T. Linden, and N. Raj, Phys. Rev. Lett. **119**, 131801 (2017), arXiv:1704.01577 [hep-ph].
 - [27] N. Raj, P. Tanedo, and H.-B. Yu, Phys. Rev. **D97**, 043006 (2018), arXiv:1707.09442 [hep-ph].
 - [28] N. F. Bell, G. Busoni, and S. Robles, JCAP **1809**, 018 (2018), arXiv:1807.02840 [hep-ph].
 - [29] R. Garani, Y. Genolini, and T. Hambye, JCAP **1905**, 035 (2019), arXiv:1812.08773 [hep-ph].
 - [30] C.-S. Chen and Y.-H. Lin, JHEP **08**, 069 (2018), arXiv:1804.03409 [hep-ph].
 - [31] K. Hamaguchi, N. Nagata, and K. Yanagi, Phys. Lett. **B795**, 484 (2019), arXiv:1905.02991 [hep-ph].
 - [32] D. A. Camargo, F. S. Queiroz, and R. Sturani, JCAP **1909**, 051 (2019), arXiv:1901.05474 [hep-ph].
 - [33] N. F. Bell, G. Busoni, and S. Robles, JCAP **1906**, 054 (2019), arXiv:1904.09803 [hep-ph].
 - [34] R. Garani and J. Heeck, Phys. Rev. **D100**, 035039 (2019), arXiv:1906.10145 [hep-ph].
 - [35] J. F. Acevedo, J. Bramante, R. K. Leane, and N. Raj, (2019), arXiv:1911.06334 [hep-ph].
 - [36] P. Montero-Camacho, X. Fang, G. Vasquez, M. Silva, and C. M. Hirata, Journal of Cosmology and Astroparticle Physics **08**, 031 (2019).
 - [37] M. Battaglieri *et al.*, in *U.S. Cosmic Visions: New Ideas in Dark Matter* (2017) arXiv:1707.04591 [hep-ph].
 - [38] J. Angle *et al.* (XENON10), Phys. Rev. Lett. **107**, 051301 (2011), [Erratum: Phys. Rev. Lett. **110**, 249901 (2013)], arXiv:1104.3088 [astro-ph.CO].
 - [39] P. Agnes *et al.* (DarkSide), Phys. Rev. Lett. **121**, 111303 (2018), arXiv:1802.06998 [astro-ph.CO].
 - [40] R. Agnese *et al.* (SuperCDMS), Phys. Rev. Lett. **121**, 051301 (2018), [Erratum: Phys. Rev. Lett. **122**, 069901 (2019)], arXiv:1804.10697 [hep-ex].
 - [41] O. Abramoff *et al.* (SENSEI), Phys. Rev. Lett. **122**, 161801 (2019), arXiv:1901.10478 [hep-ex].
 - [42] E. Aprile *et al.* (XENON), Phys. Rev. Lett. **123**, 251801 (2019), arXiv:1907.11485 [hep-ex].
 - [43] A. Aguilar-Arevalo *et al.* (DAMIC), Phys. Rev. Lett. **123**, 181802 (2019), arXiv:1907.12628 [astro-ph.CO].
 - [44] E. Aprile *et al.* (XENON), Phys. Rev. Lett. **123**, 241803 (2019), arXiv:1907.12771 [hep-ex].
 - [45] Q. Arnaud *et al.* (EDELWEISS), (2020), arXiv:2003.01046 [astro-ph.GA].
 - [46] E. Aprile *et al.* (XENON), (2020), arXiv:2006.09721 [hep-ex].
 - [47] D. Page, J. M. Lattimer, M. Prakash, and A. W. Steiner,

- Astrophys. J. Suppl. **155**, 623 (2004), arXiv:astro-ph/0403657 [astro-ph].
- [48] D. G. Yakovlev and C. J. Pethick, Ann. Rev. Astron. Astrophys. **42**, 169 (2004), arXiv:astro-ph/0402143 [astro-ph].
- [49] L. D. Landau and E. M. Lifschitz, *The Classical Theory of Fields*, COURSE OF THEORETICAL PHYSICS (Elsevier Science, 2013).
- [50] J. M. Pearson, N. Chamel, A. Y. Potekhin, A. F. Fantina, C. Ducoin, A. K. Dutta, and S. Goriely, Mon. Not. Roy. Astron. Soc. **481**, 2994 (2018), [Erratum: Mon. Not. Roy. Astron. Soc. 486, no.1, 768 (2019)], arXiv:1903.04981 [astro-ph.HE].
- [51] R. Essig, T. Volansky, and T.-T. Yu, Phys. Rev. **D96**, 043017 (2017), arXiv:1703.00910 [hep-ph].
- [52] T. Emken, R. Essig, C. Kouvaris, and M. Sholapurkar, JCAP **1909**, 070 (2019), arXiv:1905.06348 [hep-ph].
- [53] E. Aprile *et al.* (XENON), Phys. Rev. Lett. **121**, 111302 (2018), arXiv:1805.12562 [astro-ph.CO].
- [54] Z. Z. Liu *et al.* (CDEX), Phys. Rev. Lett. **123**, 161301 (2019), arXiv:1905.00354 [hep-ex].
- [55] A. Joglekar, N. Raj, P. Tanedo, and H.-B. Yu, (2020), arXiv:2004.09539 [hep-ph].
- [56] S. D. McDermott, H.-B. Yu, and K. M. Zurek, Phys. Rev. **D83**, 063509 (2011), arXiv:1011.2907 [hep-ph].
- [57] H. An, M. Pospelov, and J. Pradler, Phys. Lett. **B725**, 190 (2013), arXiv:1302.3884 [hep-ph].
- [58] J. Redondo and G. Raffelt, JCAP **1308**, 034 (2013), arXiv:1305.2920 [hep-ph].
- [59] J. H. Chang, R. Essig, and S. D. McDermott, JHEP **01**, 107 (2017), arXiv:1611.03864 [hep-ph].
- [60] E. Hardy and R. Lasenby, JHEP **02**, 033 (2017), arXiv:1611.05852 [hep-ph].
- [61] S. Knapen, T. Lin, and K. M. Zurek, Phys. Rev. **D96**, 115021 (2017), arXiv:1709.07882 [hep-ph].
- [62] T. Lin, *Proceedings, Theoretical Advanced Study Institute in Elementary Particle Physics: Theory in an Era of Data (TASI 2018): Boulder, Colorado, USA, June 4-29, 2018*, PoS **333**, 009 (2019), arXiv:1904.07915 [hep-ph].
- [63] S. Tulin and H.-B. Yu, Phys. Rept. **730**, 1 (2018), arXiv:1705.02358 [hep-ph].
- [64] G. Alvarez and H.-B. Yu, (2019), arXiv:1911.11114 [hep-ph].
- [65] D. McKeen, M. Pospelov, and N. Raj, (2020), arXiv:2006.15140 [hep-ph].
- [66] S. Reddy, *42nd Cracow School of Theoretical Physics: 42nd Course 2002: Flavor Dynamics Zakopane, Poland, May 31-June 9, 2002*, Acta Phys. Polon. **B33**, 4101 (2002), arXiv:nucl-th/0211045 [nucl-th].
- [67] R. Nan, D. Li, C. Jin, Q. Wang, L. Zhu, W. Zhu, H. Zhang, Y. Yue, and L. Qian, Int. J. Mod. Phys. **D20**, 989 (2011), arXiv:1105.3794 [astro-ph.IM].
- [68] C. Ng (CHIME Pulsar), *Pulsar Astrophysics (IAU S337)*, IAU Symp. **337**, 179 (2017), arXiv:1711.02104 [astro-ph.IM].
- [69] C. L. Carilli and S. Rawlings, *International SKA Conference 2003 Geraldton, Australia, July 27-August 2, 2003*, New Astron. Rev. **48**, 979 (2004), arXiv:astro-ph/0409274 [astro-ph].
- [70] D. Spergel *et al.*, “WFIRST-2.4: What Every Astronomer Should Know,” (2013), arXiv:1305.5425 [astro-ph.IM].